ORIGINAL PAPER

Partitioning of the grain-size components of Dali Lake core sediments: evidence for lake-level changes during the Holocene

Jule Xiao · Zhigang Chang · Bin Si ·
Xiaoguang Qin · Shigeru Itoh ·
Zaur Lomtatidze

Abstract We recovered a sediment core (DL04) from the depocenter of Dali Lake in central-eastern Inner Mongolia. The upper 8.5 m were analyzed at 1-cm intervals for grain-size distribution to partition the grain-size components and provide a high-resolution proxy record of Holocene lake level changes. Partitioning of three to six components, C1, C2, C3 through C6 from fine to coarse modes within the individual polymodal distributions, into overlapping lognormal distributions, was accomplished utilizing the method of lognormal distribution function fitting. Genetic analyses of the grain-size components suggest that two major components, C2 and C3, interpreted as offshore-suspension fine and medium-to-coarse silt, can serve as sediment proxies for past changes in the level of Dali Lake. Lower modal sizes of both C2 and C3 and greater C3 and lower C2 percentages reflect higher lake stands. The proxy data from DL04 core sediments span the last 12,000 years and indicate that Dali Lake experienced five stages during the Holocene. During the interval ca. 11,500–9,800 cal year BP, lake level was unstable, with drastic rises and falls. Following that interval, the lake level was marked by high stands between ca. 9,800 and 7,100 cal year BP. During the period from ca. 7,100 to 3,650 cal year BP, lake level maintained generally low stands, but displayed a slight tendency to rise. Subsequently, the lake level continued rising, but exhibited high-frequency, high-amplitude fluctuations until ca. 1,800 cal years ago. Since ca. 1,800 cal year BP, the lake has displayed a gradual lowering trend with frequent fluctuations.

Introduction

Since Doeglas (1946) recognized that the grain-size distributions of clastic deposits are mixtures of two or more distributions or populations, sedimentologists have made substantial efforts to separate the constituent populations using the graphical method developed by Harding (1949). The goal of this effort was to interpret the genesis of each subpopulation within a grain-size distribution and to relate different subpopulations to specific depositional processes and sedimentary environments (Inman 1949; Bagnold 1956; Folk and Ward 1957; Sindowski 1957; Tanner 1958, 1964; Moss 1962; Spencer 1963; Visher 1969;

J. Xiao (✉) · Z. Chang · B. Si · X. Qin
Key Laboratory of Cenozoic Geology and Environment,
Institute of Geology and Geophysics,
Chinese Academy of Sciences, 19 Beitucheng West Road,
Chaoyang District, Beijing 100029, China
e-mail: jlxiao@mail.iggcas.ac.cn

S. Itoh · Z. Lomtatidze
Paleo Labo Co. Ltd., Saitama 335-0016, Japan

Windom 1975). Despite great advances in the environmental interpretation of grain-size analyses, the graphical technique was considered to be subjective and imprecise and to not always yield a unique solution, particularly when applied to grain-size data of relatively low precision (Middleton 1976; Ashley 1978; Bagnold and Barndorff-Nielsen 1980).

Recently, mathematical methods were introduced to define all types of grain-size distributions and partition the grain-size components of polymodal sediments with the aid of high-resolution grain-size data generated by laser grain-size analyzers (Kranck et al. 1996a, b; Påsse 1997; Sun et al. 2002; Qin et al. 2005). By means of Weibull distribution function fitting, Sun (2004) succeeded in partitioning two grain-size components of loess deposits over the Chinese Loess Plateau, a coarse component (ca. 10–70 μm), transported mainly by the low-altitude East Asian winter monsoon, and a fine overlapping component (ca. < 10 μm), transported mainly by high-altitude westerly winds. Based on these results, Sun (2004) indicated that the winter monsoon and the northern westerlies were synchronously intensified in glacial stages and weakened in interglacial stages, and that both were strengthened progressively during the late Cenozoic. Meanwhile, Qin et al. (2005) attempted to partition the grain-size distributions of Chinese loess deposits through the fitting of lognormal distributions and came to the conclusion that the loess is composed of three sediment components, a coarse component (>10 μm), a medium component (2–10 μm), and a fine component (<2 μm). They believed that the trimodal distribution of the loess deposits resulted from the interaction of wind, atmospheric turbulence, and dust grain gravity along the dust transportation path. According to this interpretation, Qin et al. (2005) suggested that the aerodynamic environments over the dust source area during the last glaciation were mainly controlled by the strength of the winter monsoon and that eolian accumulation was closely related to the intensity of the atmospheric turbulence over the dust depositional area and the distance from dust source to dust depositional area.

The grain-size distribution of lake sediments has long been used as a proxy for a lake's hydrological conditions associated with regional climatic and environmental changes (Håkanson and Jansson 1983). Lacustrine sediments, however, are characterized by polymodal distributions, and different grain-size components within a grain-size distribution represent different sedimentary processes (Visher 1969; Middleton 1976; Ashley 1978). Therefore, grain-size parameters of lake sediments can be viewed only as approximate indicators of the hydrological conditions of lakes. In this study, we applied the mathematical method of lognormal distribution function fitting (Qin et al. 2005) to numerically partition the grain-size components within individual grain-size distributions of bulk samples taken at 1-cm intervals from the upper 8.5 m of a sediment core recovered in the depocenter of Dali Lake in central-eastern Inner Mongolia. The aim of this paper is to provide a high-resolution proxy record of fluctuations in Dali Lake level during the Holocene based on changes in the modal size and relative proportion of major grain-size components. We also propose that the approach is a valuable tool for interpreting the genesis of polymodal distributions of lake sediments and relating the grain-size components to specific sedimentary processes in lakes.

Dali Lake basin

Dali Lake (43°13′–43°23′N, 116°29′–116°45′E) is an inland, closed-basin lake that lies 90 km west of Hexigten Banner, Inner Mongolia (Fig. 1). It has an area of 238 km^2, a maximum water depth of 11 m, and an elevation of 1,226 m above sea level. The lake sits in the northern margin of the E–W trending Hulandaga Desert Land. Hills of basaltic rocks surround the lake on the north and west, and lacustrine plains are present along the eastern shore. Two permanent rivers from the northeast and two intermittent streams from the southwest enter the lake, but no rivers drain the lake (Fig. 1).

Dali Lake is located at the transition from semi-humid to semi-arid areas in the middle temperate zone of China. The climate of the lake region is controlled by the East Asian monsoon and the Westerly winds (Chinese Academy of Sciences 1984; Zhang and Lin 1992). During the winter half year, cold, dry northwesterly airflows prevail over the area and bring cold waves from late autumn to spring; whereas during the summer half year, the northward-migrating warm, moist air masses interact with cooler air from the northwest and produce most of the annual precipitation. In the lake region, mean annual

Fig. 1 Map of Dali Lake showing the location of the DL04 sediment core. Desert lands border the lake on the south; hills of basaltic rocks surround the lake on the north and west; and lacustrine plains are present along the eastern shore. Two permanent rivers from the northeast and two intermittent streams from the southwest enter the lake, but no rivers drain the lake. The bathymetric survey of the lake was conducted in June 2002 with a FE-606 Furuno Echo Sounder (contours in meters)
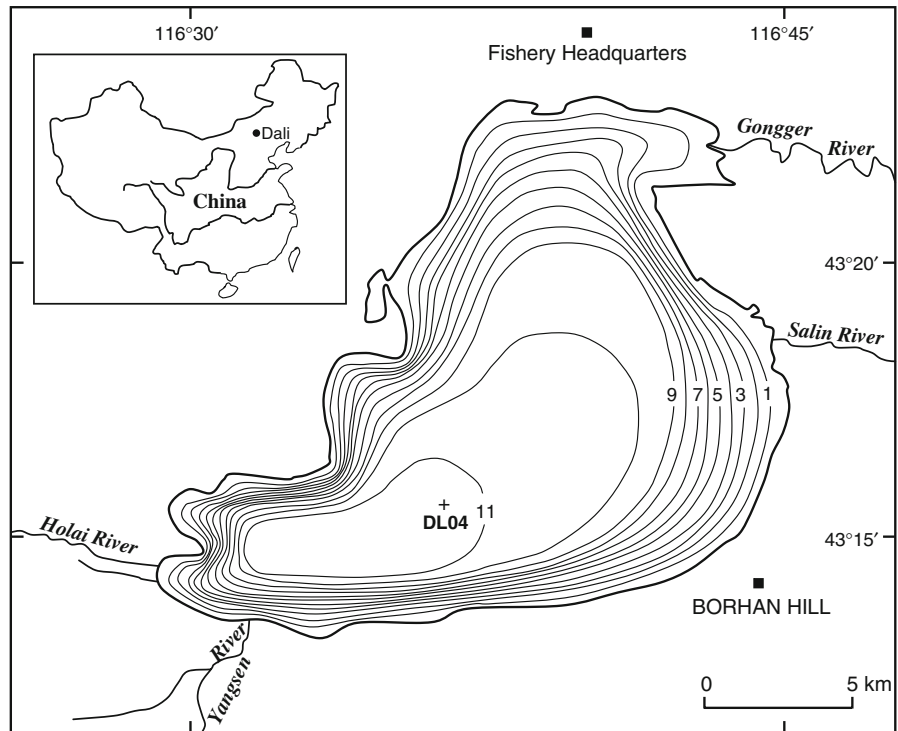
temperature is 1–2°C with a July average of 16–18°C and a January average of −17 to −24°C. Mean annual precipitation is 350–400 mm with 70% of the annual precipitation falling in June–August, and mean annual evaporation reaches 1,287 mm. The lake is covered with ca. 1 m of ice from November to April (Compilatory Commission of Annals of Hexigten Banner 1993).

Materials and methods

DL04 sediment core

In February 2004, drilling was conducted at a water depth of 10.8 m in the depocenter of Dali Lake, using a Japanese-made TOHO drilling system (Model D1–B) (Fig. 1). Sediment cores were extracted to a depth beneath the lake floor of 12.57 m, and designated DL04 (43°15.68′N, 116°36.26′E) (Fig. 1). Cores were taken in polyethylene tubes using a piston corer, and sediment recovery approached 100%. Core sections were split, photographed and described on site, and then cut into 1-cm segments for laboratory analyses. Core sediments are composed of greenish-grey to blackish-grey, homogeneous silt and silty clay

with fine laminations at core depths of 4.94–6.35 m and occasional bands at depths of 6.35–7.91 m (Fig. 2).

The upper 8.5 m of the DL04 sediment core was used for the present study and was sampled continuously, yielding 850 samples for analyses of grain-size distribution. Eighteen bulk samples were collected at ca. 50-cm intervals for radiocarbon dating from the organic-rich horizons of the upper 8.5 m of DL04 sediment core (Fig. 2).

Chronology of DL04 sediment core

Eighteen radiocarbon samples from the DL04 sediment core were dated by Accelerator Mass Spectrometry (AMS) (Compact-AMS, NEC Pelletron) at Paleo Labo Co., Ltd., Japan. Organic carbon was extracted from each sample and dated following the method described by Nakamura et al. (2000). Each sample was pretreated with an AAA process (washing with acid, alkali and acid) to remove carbonates and contaminants. After the pretreatment, the residue containing ca. 2 mg of carbon was put into a Vycor® tube together with ca. 200 mg of CuO and a few pieces of Ag wire. The tube was flame-sealed and heated to 900°C for 2 h after evacuating.
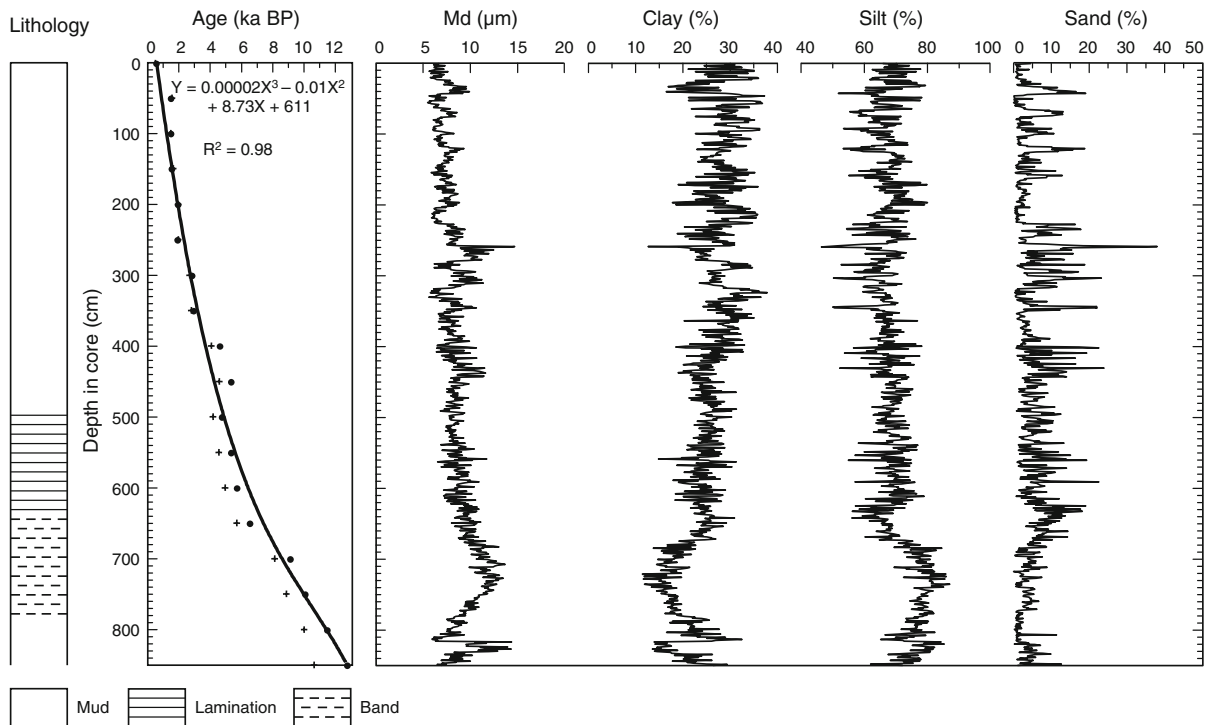
Fig. 2 Lithology, age-depth model, and grain-size distribution (Md, μm; clay, %; silt, %; sand, %) of the upper 8.5 m of DL04 sediment core recovered in the depocenter of Dali Lake. Crosses represent AMS radiocarbon ages, and dots represent calibrated radiocarbon ages with 2σ error. The age-depth model was derived by calibrated ages with a third-order polynomial fit and yields a surface-intercept age of 611 years. This age was considered to result from "hard-water" and other reservoir effects on the radiocarbon dating of the lake sediments and was subtracted from the calibrated age model when converting depth to age

The resulting CO_2 was purified in a glass vacuum line using liquid N_2, C_2H_5OH–liquid N_2 mixture ($-100°C$) and N-pentane ($-130°C$). The pure CO_2 was then converted to graphite by catalytic reduction on Fe powder.

The $^{14}C/^{12}C$ and $^{13}C/^{12}C$ ratios of each sample, with an oxalic acid standard (SRM-4990C, commonly designated HOxII), were measured with the AMS system. Each sample was measured three times, and each measurement lasted 30 min. The typical uncertainty resulting from counting statistics was 0.3%. To correct the $^{14}C/^{12}C$ ratios for isotopic fractionation, the $\delta^{13}C$ value of each sample was analyzed with the system. The background level of the AMS system, measured using a marble sample, is as low as that of a sample with an age of 50 ka.

The ^{14}C ages of all the samples from the DL04 sediment core were determined with a half-life of 5,568 years (Fig. 2; Table 1). The conventional ages were converted to calibrated ages using the OxCal3.1 radiocarbon age calibration program (Bronk Ramsey 2001) with IntCal04 calibration data (Reimer et al. 2004) (Fig. 2; Table 1).

Calibrated ages with 2σ error were used to produce an age-depth model with a third-order polynomial fit for the upper 8.5 m of the DL04 sediment core (Fig. 2). Ages of sampled horizons were calculated with the age-depth model. As shown in Fig. 2, the age-depth model yields a surface-intercept age of 611 years. This age can be considered to result from "hard-water" and other reservoir effects on the radiocarbon dating of Dali Lake sediments. Although the reservoir effects probably varied with time, in the absence of other information, we subtracted the surface intercept age from the calibrated age model when converting depth to age.

The age-depth model indicates that Holocene Epoch sediments at the site of Dali Lake core DL04 are ca. 8.3 m thick (Fig. 2). An average sedimentation rate of ca. 72 cm ka^{-1} in sediment core DL04

Table 1 AMS radiocarbon dates of samples from the upper 8.5 m of DL04 sediment core recovered in the depocenter of Dali Lake

Laboratory number	Depth interval (cm)	Dating material	$\delta^{13}C$ (‰)	AMS ^{14}C age (^{14}C yr BP $\pm 1\sigma$)	Calibrated ^{14}C age (2σ) (cal year BP)
PLD-4564	1–0	Organic matter	−28.38	470 ± 25	535–495
PLD-6249	50–49	Organic matter	−28.70	1530 ± 20	1,520–1,350
PLD-4565	100–99	Organic matter	−25.62	1460 ± 25	1,390–1,300
PLD-6250	150–149	Organic matter	−28.24	1625 ± 20	1,570–1,410
PLD-4567	200–199	Organic matter	−24.76	1945 ± 25	1,950–1,820
PLD-6251	250–249	Organic matter	−30.34	1930 ± 20	1,930–1,820
PLD-4568	300–299	Organic matter	−25.82	2695 ± 25	2,850–2,755
PLD-6252	350–349	Organic matter	−25.56	2805 ± 20	2,970–2,850
PLD-4570	400–399	Organic matter	−26.24	4080 ± 25	4,650–4,510
PLD-6253	450–449	Organic matter	−26.16	4580 ± 25	5,330–5,280
PLD-4571	500–499	Organic matter	−27.21	4180 ± 25	4,770–4,620
PLD-6706	550–549	Organic matter	−23.77	4560 ± 20	5,320–5,270
PLD-4572	600–599	Organic matter	−27.41	4945 ± 30	5,730–5,600
PLD-6255	650–649	Organic matter	−25.72	5705 ± 25	6,570–6,410
PLD-4573	700–699	Organic matter	−29.34	8105 ± 35	9,130–8,990
PLD-6256	750–749	Organic matter	−25.62	8865 ± 30	10,170–9,860
PLD-4574	800–799	Organic matter	−28.10	9995 ± 40	1,1630–11,270
PLD-6257	850–849	Organic matter	−30.50	10640 ± 35	12,810–12,620

indicates that a sampling interval of 1 cm provides temporal resolution of ca. 14 year.

Grain-size distribution of DL04 core sediments

Grain-size distribution of 850 samples was determined with a Malvern Mastersizer 2000 laser grain-size analyzer. About 200 mg of sediment from each air-dried, disaggregated sample was pretreated with 10–20 ml of 30% H_2O_2 to remove organic matter and then with 10 ml of 10% HCl with the sample solution boiled to remove carbonates. About 2,000 ml of deionized water was added, and the sample solution was kept for ca. 24 h to rinse acidic ions. The sample residue was dispersed with 10 ml of 0.05 M $(NaPO_3)_6$ on an ultrasonic vibrator for 10 min before grain-size analysis.

The Mastersizer 2000 works on the principle of the Mie theory that predicts the way light is scattered by spherical particles and deals with the way light passes through, or is absorbed by, the particle. Because each particle size has its own characteristic scattering pattern, the Mastersizer can calculate the size of particles that create a pattern by using the optical unit to capture the scattering pattern from a field of particles. Based on the Mie theory, assuming that measured particles are perfect spheres, the Mastersizer uses the volume of a particle to measure its size and calculate the diameter of an imaginary sphere that is equivalent in volume by the technique of "equivalent spheres." The Mastersizer 2000 has a measurement range of 0.02–2,000 μm in diameter and a grain-size resolution of 0.166 Φ in interval, thus yielding 100 pairs of grain-size data. Duplicate analyses of the same sample showed that the relative error of percentages of the related size fractions is less than 1%. It automatically outputs the median diameter (Md, the diameter at the 50th percentile of the distribution) and the percentages of clay, silt and sand fractions of a sample. These data (Md, μm; clay, %; silt, %; sand, %) of the upper 8.5 m of DL04 core sediments were plotted against depth in core in Fig. 2.

Identifying, fitting and partitioning of the grain-size components

Figure 3 shows representative grain-size distributions from 850 consecutive 1-cm sections from the upper 8.5 m of the DL04 sediment core. The data indicate that Dali Lake sediments consist of a strongly

polymodal mixture of different grain-size components, including clay, silt and sand (Fig. 3).

It has been suggested that the grain-size distribution of clastic deposits with a single component formed by only one process should exhibit a symmetric curve on a logarithmic scale and represent a unimodal distribution (Inman 1949; Folk and Ward 1957; Tanner 1964; Visher 1969; Ashley 1978). When the shape of the grain-size distribution is asymmetric or skewed, the total distribution can be considered to be a combination of several unimodal distributions formed by different processes (Inman 1949; Folk and Ward 1957; Tanner 1964; Visher 1969; Ashley 1978). In other words, a polymodal grain-size distribution is composed of two or more unimodal grain-size components. As shown in Fig. 3, each polymodal distribution of samples from Dali Lake sediments can be thought of as composed of two or more unimodal distributions representing two or more grain-size components (modes), respectively.

The concept that the grain-size distribution of unimodal clastic deposits follows the lognormal distribution (Krumbein 1938) has been widely adopted. It has been suggested that the lognormal distribution function gives sufficient accuracy in describing unimodal grain-size distributions (Ashley 1978; Påsse 1997). In the present study, the grain-size components of individual polymodal distributions were identified, fitted and partitioned using the lognormal distribution function method described by Qin et al. (2005).

This method assumes that a polymodal or skewed grain-size distribution is composed of two or more unimodal lognormal distributions. The prototype formula of the lognormal function is as follows,

$$F(x) = \sum_{i=1}^{n} \left[\frac{c_i}{\sigma_i \sqrt{2\pi}} \int_{-\infty}^{\infty} \exp\left(-\frac{(x - a_i)^2}{2\sigma_i^2} \right) dx \right]$$

where n is the number of modes, $x = \ln(d)$, d is the grain size in μm, c_i is the content of the ith mode, σ_i is the variance of the ith mode, and a_i is the mean value of the ith mode's logarithm grain size, i.e., $a_i = \ln(d_i)$.

The residual error is calculated as,

$$dF = \frac{1}{m} \sum_{j=1}^{m} \left(F(x_j) - G(x_j) \right)^2$$

where m is the number of grain-size intervals and $G(x)$ is the measured grain-size distribution of a sample. To estimate the fitting parameters, a combination (n, c_i, a_i, σ_i) of three parameters of n modes with minimum residual error dF is chosen to represent the polymodal distribution, by iteratively changing each parameter in a shorter step.

Fitting experiments on the same sample are accomplished when the residual error is <4. Numerical partitioning of the unimodal components can be achieved simultaneously through lognormal distribution function fitting because the parameters and the distribution functions of each component are determined during fitting. The modal sizes and relative percentages of each component are given as soon as the fitting is accomplished.

Fitting experiments on 850 samples from the upper 8.5 m of DL04 sediment core demonstrate that the lognormal distribution function yields the best fitting results from most of the samples with the squared sum of residual error <2.

Characteristics of the grain-size components

Fittings of the lognormal distribution function suggest that each polymodal distribution of samples from Dali Lake sediments consists of three to six unimodal distributions representing three to six grain-size components (modes), respectively. In this study, the six components are designated C1, C2, C3 through C6 from fine to coarse modes (Fig. 3).

As shown in Fig. 3, it is easy to determine the modes of components C1, C4, C5 and C6. To separate out components C2 and C3, however, requires technical skills through trial-and-error fittings after careful observations, because both components strongly overlap. In this case, fortunately, the fitting residual error increases significantly if either the C2 (negative skew) or C3 (positive skew) is ignored. Such experiments demonstrate the validity and accuracy of the lognormal distribution function applied to fitting and partitioning the grain-size components within individual grain-size distributions of polymodal lake sediments.

Grain-size data suggest that components C1, C2, C3 through C6 identified from 850 individual grain-size distributions of Dali Lake sediments have identifiable characteristics (Figs. 4, 5; Table 2). All the samples contain the components C1 and C2, while 88 (10%) samples from different horizons lack the C3, and the C4, C5 and C6 exist only in 263
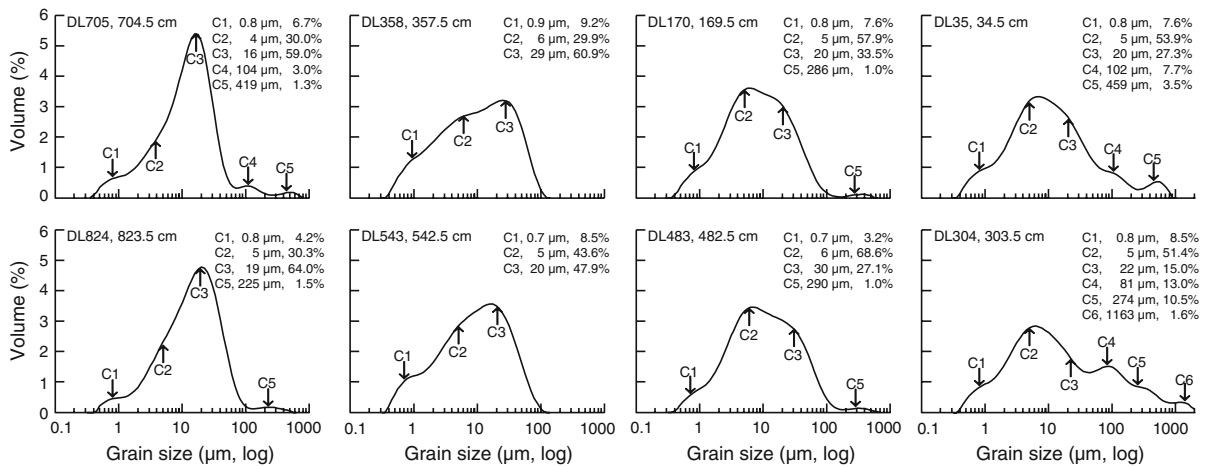
Fig. 3 Representative frequency curves of the grain-size distributions of 850 samples from the upper 8.5 m of DL04 sediment core. In each diagram, capital letters DL with numerals indicate the sample number, followed by the depth of the sampled horizon. Altogether, six grain-size components can be recognized on the polymodal distributions, and are designated C1 through C6 from fine to coarse modes. The components of each sample were marked on the frequency curve, and the modal sizes and relative percentages of each component were shown on the upper-right of each diagram

(31%), 290 (34%) and 71 (8%) samples, respectively. The modal sizes of the components C1, C2, C3 through C6 vary primarily within ranges of 0.7–1.0, 4.2–8.1, 10.9–60.2, 66.8–104.1, 197.1–470.4 and 944.4–1074.8 μm, respectively. The relative percentages of the C1, C4, C5 and C6 vary primarily within ranges of 2.3–12.8%, 0.3–13.7%, 0.1–5.0% and 0.4–3.3%, respectively; whereas both the C2 and the C3 display two dominant ranges of the relative percentages, i.e., 21.1–38.3% as well as 55.5–95.5%, and 0.5–36.1% as well as 46.2–71.6%. Finally, when the C4 appears in samples, either the C3 is absent, or the C3 displays a modal size of less than ca. 50 μm.

Discussion

Interpretation of the grain-size components

Dali Lake is located on the northern margin of the E–W trending Hulandaga Desert Land. There are two permanent rivers and two intermittent streams entering the lake. In terms of the geographic location and basin structure, clastic sediments in Dali Lake would be expected to derive from three sources through distinct transport mechanisms, i.e., fluvial materials transported by the rivers and streams, eolian deposits blown by winds, and shoreline materials eroded by storm-driven waves. Clastic materials from the three sources are deposited on the lake floor after being reworked and sorted by the hydraulic conditions of lake water (Håkanson and Jansson 1983).

Detailed studies of grain-size distributions suggested that the three types of clastic sediments exhibit different combinations of specific grain-size components. Fluvial sediments are composed mainly of two grain-size components, i.e., a saltation medium-sand component with dominant modal sizes of 200–400 μm and a suspension fine-silt component with dominant modal sizes of 10–15 μm (Middleton 1976; Ashley 1978; Bennett and Best 1995). Grain-size components of eolian deposits depend on the nature of winds (i.e., high- and low-altitude air flows and near-ground winds) and transport distances (long or short distance) (Pye 1987; Tsoar and Pye 1987; Sun et al. 2002). Typical loess deposits consist of a short-suspension, medium-to-coarse silt component with dominant modal sizes of 16–32 μm and a long-suspension clay-to-fine silt component with dominant modal sizes of 2–6 μm (Pye 1987; Tsoar and Pye 1987; Sun et al. 2002; Qin et al. 2005); whereas desert sands mainly consist of a saltation component of fine-to-medium sands with dominant modal sizes of 100–200 μm and a suspension component of clay-to-fine silt with dominant modal sizes of 2–6 μm (Gillette et al. 1974; Pye 1987; Tsoar and Pye 1987; Sun et al. 2002). Lake shoreline materials are dominantly composed of unconsolidated sands
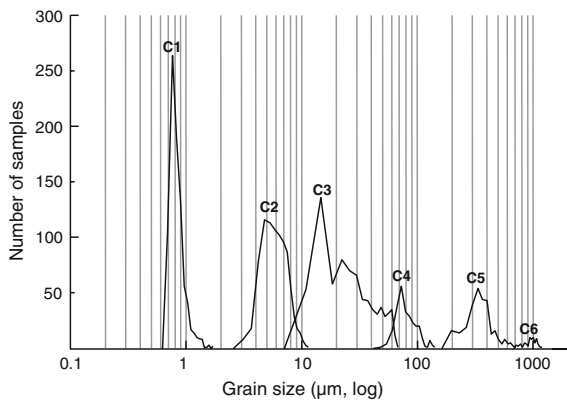
Fig. 4 Frequencies of the modal sizes of the six grain-size components, C1 through C6, in 850 samples from the upper 8.5 m of DL04 sediment core
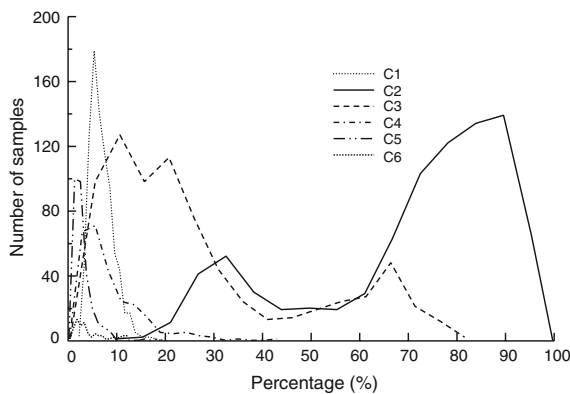

Fig. 5 Frequencies of the relative percentages of the six grain-size components, C1 through C6, in 850 samples from the upper 8.5 m of DL04 sediment core

with a low proportion of silty clay (Sly 1978; Håkanson and Jansson 1983). The grain-size components of lake sediments would have been derived from the three

types of clastic deposits; however, the combination of the grain-size components and the characteristics of each component such as the modal size and relative percentage would be highly modified by the processes of transportation and deposition in lake water.

Deposition of clastic materials in lakes is controlled mainly by hydraulic conditions (Sly 1978; Håkanson and Jansson 1983). Fundamentally, there exists a relationship between clastic and hydraulic interactions, so that lake sediments can be separated into high and low hydraulic energy regimes (Sly 1978; Håkanson and Jansson 1983; Sly 1989a, b). In general, the nearshore zone of lakes lies in higher energy environments than the offshore zone does, and deposits of decreasing particle size towards the depocenter of lakes reflect decreasing hydraulic energy. Grain-size distributions of 51 samples collected from the surface sediments of Dali Lake indicate that (1) components C4, and especially C5 and C6 appear in all nearshore samples, but are lacking in offshore samples; (2) the relative percentage of the components C2 plus C3 is considerably higher in the offshore samples than in the nearshore ones; and (3) component C1 exists in all samples from both the offshore and nearshore zones, albeit at relatively low percentages.

Using spatial changes in the dominant grain-size components of the surface sediments, together with the dominant modal sizes of fluvial, eolian and lake shoreline deposits, we inferred that grain-size components C1, C2, C3 through C6 of Dali Lake sediments represent different sedimentary modes related to different hydraulic regimes (Table 2). Components C2 and C3, with dominant modal sizes ranging from 4.2 to 8.1 μm and 10.9 to 60.2 μm, respectively, represent two offshore suspension

Table 2 Characteristics of the six grain-size components recognized on the polymodal distributions of samples from the DL04 core sediments

Component	Number of samples	Modal size (μm)		Dominant range of modal sizes (μm)	Percentage		Dominant range of percentages	Description of the components
		Min.	Max.		Min.	Max.		
C1	850	0.7	1.7	0.7–1.0	2.3	18.0	2.3–12.8	Long-term suspension
C2	850	2.9	11.1	4.2–8.1	9.6	95.5	21.1–38.3, 55.5–95.5	Offshore suspension
C3	762	9.0	65.9	10.9–60.2	0.5	76.8	0.5–36.1, 46.2–71.6	Offshore suspension
C4	263	47.2	140.5	66.8–104.1	0.3	40.5	0.3–13.7	Nearshore suspension
C5	290	180.9	693.5	197.1–470.4	0.1	18.3	0.1–5.0	Nearshore saltation
C6	71	701.4	1190.3	944.4–1074.8	0.4	11.5	0.4–3.3	Nearshore traction

components. Components C4, C5 and C6, with dominant modal sizes of 66.8–104.1, 197.1–470.4 and 944.4–1074.8 μm, respectively, are interpreted as nearshore suspension, saltation, and traction components, respectively. Component C1, finer than 2 μm, may belong to the long-term suspension component in fluid medium, the movement and deposition of which depend on the intensity of turbulence.

It has been suggested that high-energy sedimentary processes are less significant in lake environments, particularly in small basins (Håkanson and Jansson 1983; Sly 1989a, b). Assuming this is the case, the relative percentages of the six grain-size components led us to conclude that C2 and C3 would be the major components of Dali Lake sediments and that changes in the modal size and relative percentage of C2 and C3 would be closely associated with the hydraulic conditions in the lake.

Implication of major grain-size components

Hydraulic conditions in lakes are related to water depth, shape, size, and the surrounding relief (Håkanson and Jansson 1983; Sly 1989a, b). The shallow water of the nearshore zone possesses higher energy than the offshore, deep-water zone. Particle size of the sediments decreases with greater depth and declining hydraulic energy (Håkanson and Jansson 1983; Sly 1989a, b). In Dali Lake, components C2 and C3 should become fine during periods of high lake levels. Thus, modal sizes of C2 and C3 can be used as proxies for the level of Dali Lake. Low modal sizes of C2 and C3 reflect high lake levels.

Modal sizes of components C3 (9.0–65.9 μm) and C4 (47.2–140.5 μm) overlap (Figs. 3, 4; Table 2), implying an inherent relation between C3 and C4. On one hand, components C3 and finer C4 may have been derived from the short-suspension, medium-to-coarse silt component of eolian deposits, according to the range of the modal sizes. On the other hand, the C3 could have been reworked to finer C4 under specific hydraulic conditions of lake water, because whenever the C3 was absent from samples, the C4 was present. We speculate that changes in the relative percentage of component C3 might have been related to changes in the hydraulic energy regime of the lake. Greater proportions of the C3 could be reworked to the C4, resulting in decreasing relative percentages of the C3, under higher hydraulic energies when the lake

level was lower. In other words, the percentage of C3 can be linked to lake levels, with high percentages of C3 generally denoting high lake levels. The fact that high percentages of the C3 coincide with low modal sizes of C2 and C3 (Fig. 6) lends support to such an inference that high percentages of C3 indicate high lake levels. In addition, the relative percentages of component C2 display a strongly negative correlation with those of C3 (Fig. 6), presumably implying that the proportion of C2 decreases during the periods of high lake levels when that of the C3 increases. In summary, low modal sizes of both components C2 and C3, and high C3 and low C2 percentages, would reflect high levels of Dali Lake.

Lake-level changes during the Holocene

The modal sizes of components C2 (C2MS, μm) and C3 (C3MS, μm), and percentages of C2 and C3 from DL04 core sediments spanning the last ca. 12,000 years were plotted against calibrated radiocarbon ages (Fig. 6). The data indicate that stage changes of Dali Lake during the Holocene can be divided into five major stages (Fig. 6). During the interval from ca. 11,500 to 9,800 cal year BP, the lake level was unstable, with drastic rises and falls. Following that interval, the lake level was marked by high stands between ca. 9,800 and 7,100 cal year BP. During the period from ca. 7,100 to 3,650 cal year BP, the lake level was generally low, but displayed a slight tendency to rise. Subsequently, the lake level continued rising, but exhibited high-frequency, high-amplitude fluctuations until ca. 1,800 cal years ago. Since ca. 1,800 cal year BP, the lake has gradually shrunk, with frequent stage fluctuations.

Proxy data of total organic and inorganic carbon (TOC and TIC) concentrations from DL04 core sediments also revealed a detailed history of stage changes in Dali Lake during the Holocene (Xiao et al. 2008). High TOC and low TIC concentrations indicate that Dali Lake reached its highest level during the early Holocene (11,500–7,600 cal year BP). The middle Holocene (7,600–3,450 cal year BP) was characterized by dramatic fluctuations in the lake level with three intervals of lower lake stands occurring 6,600–5,850, 5,100–4,850 and 4,450–3,750 cal year BP, respectively. During the late Holocene (3,450 cal year BP to present), general increases in TIC and decreases in TOC reflect a

gradual shrinking trend of Dali Lake. These data provide support for our inference of changes in the lake level of Dali Lake during the Holocene based on the grain-size components identified from the lake sediments.

Xiao et al. (2008) inferred that the expansion of Dali Lake during the early Holocene, before ca. 7,600 cal year BP, resulted from the meltwater input of the snow/ice packs covering the high mountains in the upper reaches of the Gongger River, in response to the increase in summer solar radiation in the Northern Hemisphere. We concur with this inference. The modal size and relative percentages of components C2 and C3 between ca. 9,800 and 7,100 cal year BP are different from those after ca. 7,100 cal year BP, both in magnitude and amplitude (Fig. 6). This striking contrast may imply that the mechanism responsible for this early rise in lake level is unique within the Holocene. During the early Holocene, a large quantity of water from melting of the snow/ice packs discharged into the lake, leading to a rapid rise in lake level. Rapid expansion of the lake left the core location in the depocenter of the lake farther from the lakeshore, resulting in a stable regime of low hydraulic energies for the deposition of fine clastic materials. Grain-size components of Dali Lake sediments provide further evidence for the inference that the early Holocene high stand can be attributed to input of the snow/ice melt.

Conclusions

Application of the lognormal distribution function method in fitting and partitioning the grain-size components within individual distributions suggests that strongly polymodal Dali Lake sediments consist of three to six overlapping components. Genetic analyses of the grain-size components indicate that each of the components retains its identity (modal size, manner of transportation and environment of deposition) even though the relative proportions vary with the hydrological conditions throughout the lake.

Two major grain-size components (C2 and C3), interpreted as offshore deposits of suspended fine and medium-to-coarse silt, can serve as proxies for stage change in Dali Lake. Lower modal sizes of both C2 and C3, and greater C3 and lower C2 percentages
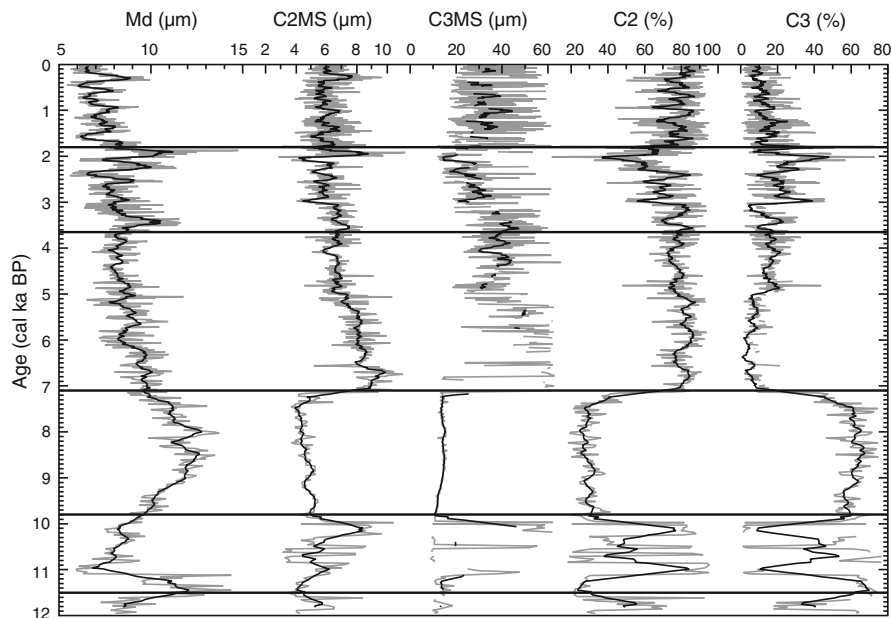

Fig. 6 Median grain size of bulk samples (Md, µm), modal sizes of the components C2 (C2MS, µm) and C3 (C3MS, µm), and relative percentages of the C2 (%) and C3 (%) from DL04 core sediments spanning the last 12,000 years. The chronology for the DL04 sediment core was derived from the age-depth model with the surface-intercept age subtracted. Bold lines superimposed on the data plots represent nine-point running means. The lower horizontal solid line marks the onset of the Holocene, and the upper ones bracket the stages characterizing the pattern of changes in the lake level of Dali Lake. Low modal sizes of both C2 and C3, and great C3 and low C2 percentages indicate high lake levels

reflect higher lake stands. The data indicate that Dali Lake experienced five stages during the Holocene: (1) unstable, with drastic rises and falls during the interval of ca. 11,500–9,800 cal year BP, (2) stable high stands between ca. 9,800 and 7,100 cal year BP, (3) low stands with a slight tendency to rise from ca. 7,100 to 3,650 cal year BP, (4) continuing rises with high-frequency, high-amplitude fluctuations until ca. 1,800 cal year BP, and (5) a gradual decline with frequent fluctuations during the last 1,800 cal years.

The apparent success of the lognormal distribution function method in fitting and partitioning polymodal grain-size distributions of lake sediments should prove to be a powerful tool for understanding the sedimentary processes of clastic materials in lake systems and for interpreting environmental conditions around lakes.

References

Ashley GM (1978) Interpretation of polymodal sediments. J Geol 86:411–421

Bagnold RA (1956) The flow of cohesionless grains in fluids. Philos Trans R Soc Lond 249:235–297. doi:10.1098/rsta.1956.0020

Bagnold RA, Barndorff-Nielsen O (1980) The pattern of natural size distributions. Sedimentology 27:199–207. doi:10.1111/j.1365-3091.1980.tb01170.x

Bennett SJ, Best JL (1995) Mean flow and turbulence structure over fixed, two-dimensional dunes: implications for sediment transport and bedform stability. Sedimentology 42:491–513. doi:10.1111/j.1365-3091.1995.tb00386.x

Bronk Ramsey C (2001) Development of the radiocarbon calibration program. Radiocarbon 43:355–363

Chinese Academy of Sciences (Compilatory Commission of Physical Geography of China) (1984) Physical geography of China: climate. Science Press, Beijing, pp 1–30 (in Chinese)

Compilatory Commission of Annals of Hexigten Banner (1993) Annals of Hexigten Banner. People's Press of Inner Mongolia, Hohhot, pp 97–104, 550–551 (in Chinese)

Doeglas DJ (1946) Interpretation of the results of mechanical analyses. J Sediment Petrol 16:19–40

Folk RL, Ward WC (1957) Brazos River bar: a study in the significance of grain size parameters. J Sediment Petrol 27:3–26

Gillette DA, Blifford DA, Fryear DW (1974) The influence of wind velocity on size distributions of soil wind aerosols. J Geophys Res 79:4068–4075. doi:10.1029/JC079i027p04068

Håkanson L, Jansson M (1983) Principles of lake sedimentology. Springer, Berlin, p 316

Harding JP (1949) The use of probability paper for the graphical analysis of polymodal frequency distributions. J Mar Biol Assoc UK 28:141–153

Inman DL (1949) Sorting of sediments in the light of fluid mechanics. J Sediment Petrol 19:51–70

Kranck K, Smith PC, Milligan TG (1996a) Grain-size characteristics of fine-grained unflocculated sediments I: 'one-round' distributions. Sedimentology 43:589–596. doi:10.1046/j.1365-3091.1996.d01-27.x

Kranck K, Smith PC, Milligan TG (1996b) Grain-size characteristics of fine-grained unflocculated sediments II: 'multi-round' distributions. Sedimentology 43:597–606. doi:10.1046/j.1365-3091.1996.d01-28.x

Krumbein WC (1938) Size frequency distribution of sediments and the normal phi curve. J Sediment Petrol 8:84–90

Middleton GV (1976) Hydraulic interpretation of sand size distributions. J Geol 84:405–426

Moss AJ (1962) The physical nature of common sandy and pebbly deposits, part I. Am J Sci 260:337–373

Nakamura T, Niu E, Oda H, Ikeda A, Minami M, Takahashi H, Adachi M, Pals L, Gottdang A, Suya N (2000) The HVEE Tandetron AMS system at Nagoya University. Nucl Instrum Methods Phys Res B B172:52–57

Påsse T (1997) Grain size distribution expressed as *tanh*-functions. Sedimentology 44:1011–1014

Pye K (1987) Aeolian dust and dust deposits. Academic Press, London, pp 29–62

Qin XG, Cai BG, Liu TS (2005) Loess record of the aerodynamic environment in the East Asia monsoon area since 60,000 years before present. J Geophys Res 110:B01204. doi:10.1029/2004JB003131

Reimer PJ, Baillie MGL, Bard E, Bayliss A, Beck JW, Bertrand CJH, Blackwell PG, Buck CE, Burr GS, Cutler KB, Damon PE, Edwards RL, Fairbanks RG, Friedrich M, Guilderson TP, Hogg AG, Hughen KA, Kromer B, McCormac G, Manning S, Bronk Ramsey C, Reimer RW, Remmele S, Southon JR, Stuiver M, Talamo S, Taylor FW, van der Plicht J, Weyhenmeyer CE (2004) Intcal04 terrestrial radiocarbon age calibration, 0–26 cal kyr BP. Radiocarbon 46:1029–1058

Sindowski KH (1957) Die synoptische Methode des Kornkurven-Vergleiches zur Ausdeutung fossiler Sedimentationsräume. Geol Jahrb 73:235–275

Sly PG (1978) Sedimentary processes in lakes. In: Lerman A (ed) Lakes: chemistry, geology, physics. Springer, New York, pp 65–89

Sly PG (1989a) Sediment dispersion: part 1, fine sediments and significance of the silt/clay ratio. Hydrobiologia 176/177:99–110. doi:10.1007/BF00026547

Sly PG (1989b) Sediment dispersion: Part 2, characterisation by size of sand fraction and per cent mud. Hydrobiologia 176/177:111–124. doi:10.1007/BF00026548

Spencer DW (1963) The interpretation of grain size distribution curves of clastic sediments. J Sediment Petrol 33:180–190

Sun DH (2004) Monsoon and westerly circulation changes recorded in the late Cenozoic aeolian sequences of

Northern China. Glob Planet Change 41:63–80. doi:10.1016/j.gloplacha.2003.11.001

Sun DH, Bloemendal J, Rea DK, Vandenberghe J, Jiang FC, An ZS, Su RX (2002) Grain-size distribution function of polymodal sediments in hydraulic and aeolian environments, and numerical partitioning of the sedimentary components. Sediment Geol 152:263–277. doi:10.1016/S0037-0738(02)00082-9

Tanner WF (1958) The zig-zag nature of type I and type IV curves. J Sediment Petrol 28:372–375

Tanner WF (1964) Modification of sediment size distributions. J Sediment Petrol 34:156–164

Tsoar H, Pye K (1987) Dust transport and the question of desert loess formation. Sedimentology 34:139–153. doi:10.1111/j.1365-3091.1987.tb00566.x

Visher GS (1969) Grain size distributions and depositional processes. J Sediment Petrol 39:1074–1106

Windom HL (1975) Eolian contributions to marine sediments. J Sediment Petrol 45:520–529

Xiao JL, Si B, Zhai DY, Itoh S, Lomtatidze Z (2008) Hydrology of Dali Lake in central-eastern Inner Mongolia and Holocene East Asian monsoon variability. J Paleolimnol 40:519–528

Zhang JC, Lin ZG (1992) Climate of China. Wiley, New York, p 376